JOC The Journal of Organic Chemistry

Article

Cite This: J. Org. Chem. 2017, 82, 11464-11473

pubs.acs.org/joc

Mechanistic Insight into the Cu-Catalyzed C−S Cross-Coupling of Thioacetate with Aryl Halides: A Joint Experimental−Computational Study

Silvia M. Soria-Castro,[†] Diego M. Andrada,[*,‡,§] Daniel A. Caminos,[†] Juan E. Argüello,[†] Marc Robert,[∥] and Alicia B. Peñéñory[*,†]

[†]Departamento de Química Orgánica, Facultad de Ciencias Químicas, INFIQC, Universidad Nacional de Córdoba, CONICET, X5000HUA Córdoba, Argentina

[‡]Philipps-Universität Marburg, Fachbereich Chemie, Hans-Meerwein straße 4, 35032 Marburg, Germany

[§]Krupp-Professur für Allgemeine und Anorganische Chemie, Universität des Saarlandes, 66123 Saarbrücken, Germany

[∥]Laboratoire d'Electrochimie Moléculaire, UMR 7591 CNRS, Université Paris Diderot, Sorbonne Paris Cité, 15 rue Jean-Antoine de Baïf, F-75205 Paris Cedex 13, France

Supporting Information

ABSTRACT: The mechanism of the Ullmann-type reaction between potassium thioacetate (KSAc) and iodobenzene (PhI) catalyzed by CuI associated with 1,10-phenanthroline (phen) as a ligand was explored experimentally and computationally. The study on C−S bond formation was investigated by UV−visible spectrophotometry, cyclic voltammetry, mass spectrometry, and products assessment from radical probes. The results indicate that under experimental conditions the catalytically active species is [Cu(phen)(SAc)] regardless of the copper source. An examination of the aryl halide activation mechanism using radical probes was undertaken. No evidence of the presence of radical species was found during the reaction process, which is consistent with an oxidative addition cross-coupling pathway. The different reaction pathways leading to the experimentally observed reaction products were studied by DFT calculation. The oxidative addition−reductive elimination mechanism via an unstable Cu^{III} intermediate is energetically more feasible than other possible mechanisms such as single electron transfer, halogen atom transfer, and σ-bond methatesis.

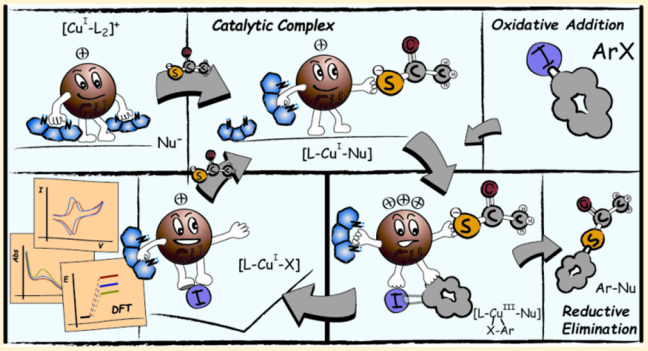

INTRODUCTION

The C−S bond-formation reactions have attracted widespread attention as a tool to construct highly relevant molecules with applications in biological, pharmaceutical, and material areas.[1] Among conventional approaches, the use of metals has been developing rapidly after overcoming the mismatch with sulfur containing compounds.[2] In particular, Ullmann cross-coupling copper-mediated reactions have proven to be an efficient and environmentally friendly alternative pathway for building this desired motif.[1a] For a long time, these processes have been far from reaching reliability, mildness, functional group tolerance, and selectivity.[1f,3] However, the successful achievements of improved catalytic strategies have triggered a "renaissance" of what is now known as the modified Ullmann reaction.[3,4] Arguably, the use of auxiliary ligands (L), often bidentate ligands such as phenanthroline,[5] diamines,[6] amino acids,[3d,7] and β-ketoesters,[8] among others,[9] turned out to be the key to broaden the scope of this chemistry.[4a] However, despite extensive studies to set synthetic strategies, no comparable effort has been made to elucidate the reaction mechanisms under different reaction conditions.[2b,3b,10]

For more than half a century, many mechanisms have been proposed to explain the C−X (X = N, O, and S) bond formation.[11,12] While the related Ullmann-type C−N and C−O bond formation reactions have been widely explored and reasonably understood, the corresponding C−S formation has had significantly less insight.[2a,b,3b,13] Due to the various possible intermediates and the different oxidation and copper coordination states, the operating mechanism remains under discussion. Currently accepted mechanisms can be summarized in four different alternatives, namely oxidative addition/reductive elimination (OA/RE),[10d,14,15] single electron transfer (SET), halogen atom transfer (HAT),[10d,16,17] and metathesis of σ-bond,[14b,18] while alternatives have also been proposed.[11a,19] In the recent past, several examples were reported for the oxidative addition of the aryl halide (ArI) to a copper complex

Received: August 7, 2017
Published: September 29, 2017

DOI: 10.1021/acs.joc.7b01991
J. Org. Chem. 2017, 82, 11464−11473

[(L)Cu(SAr)]. Elusive mechanism proposal includes the formation of an [(L)Cu^{III}(SAr)IAr] intermediate, which may then lead to the desired product through a reductive elimination.[10a−c] In this context, Cheng et al. in 2011 reported the first experimental hints by the observation of the reactive intermediate using in situ electrospray ionization mass spectrometry under catalytic reaction conditions.[20] On the basis of those results, the catalytic OA/RE where no auxiliary ligand is involved was proposed. Later, Chen et al. described the synthesis and isolation of [(phen)Cu(μ-SAr)]$_2$ dimer complexes in THF, which can react with iodoarenes.[15d] On the basis of reactivity studies, they provided evidence against the SET and HAT mechanisms. However, Zhang et al. recently carried out the first theoretical study on the mechanism of the Cu-catalyzed *S*-arylation reaction of iodobenzene using 1,10-phenanthroline in toluene, and by a thorough examination, they claimed that the HAT mechanism from PhI to the active [LCu(SAr)] species is the most likely pathway.[21] Shortly after, Weng et al. reported preparation and isolation of a series of trifluoromethylthiolate complexes ligated by bipyridine ligands.[22] They demonstrated that these complexes can react with aryl and heteroaryl halides to afford trifluoromethylthioesthers. Computational studies performed therein led to the suggestion of an OA/RE pathway.

We recently developed a simple and economical protocol to synthesize a variety of thioacetates and sulfur heterocycles by means of copper-catalyzed cross-coupling reaction under conventional and microwave conditions.[23] Continuing our research in this area, we were interested in contributing to clarify the reaction mechanism. Given the scarce studies on sulfur nucleophiles, we chose the coupling reaction between PhI and potassium thioacetate salt KSAc (**1**) catalyzed by copper in the presence of 1,10-phenanthroline (phen) as ligand (Scheme 1). Herein,

Scheme 1. Cu-Catalyzed C−S Cross Coupling Reaction of 1 with Iodobenzene

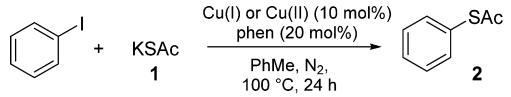

phen = 1, 10-phenanthroline

we present a combined experimental and computational study in an effort to understand the underlying mechanism of these transformations. We report an electrochemical and spectroscopic characterization of different Cu/L/Nu species involved. Additionally, experiments were designed to obtain evidence on the possible reactive intermediates, and we further performed a DFT computational study on the possible pathways.

RESULTS AND DISCUSSION

Formation of Active Cu^{I} Species from Cu^{II} Precursors. It has been observed that the formation of C−O and C−N bonds catalyzed by Cu^{II} species are slower than those catalyzed by Cu^{I}, which suggests that a prior reaction takes place in which the Cu^{II} precursor slowly releases an active Cu^{I} catalyst.[10d] It has also been shown by UV−visible absorption spectrophotometry that the Cu^{II} species coordinated with phen can be reduced in situ by alcohols or amines, in the presence of a base, to generate Cu^{I} active species.[12b]

However, in the case of the formation of C−S bonds, it has not yet been proven that the formation of active Cu^{I} species from Cu^{II} precursors occurs under experimental conditions. We previously established that CuI and CuCl exhibited similar catalytic activity as well as Cu^{II} chloride dihydrated salt ($CuCl_2.2H_2O$) during the formation of *S*-aryl thioacetates while using phen as ligand (Scheme 1).[23a] To monitor the Cu^{II}/Cu^{I} conversion mediated by a sulfur nucleophile, we first performed cyclic voltammetry experiments. The auxiliary ligand used in the reaction model, phen, can complex both Cu^{I} and Cu^{II} species. During CV study of the complex [Cu^{II}(phen)$_2$]$^{2+}$, signals corresponding to Cu^{I} species were observed, even before the addition of the ligand and the sulfur nucleophile. Many control CV experiments were performed; in all cases, we observed the same behavior.

Consequently, UV−visible absorption spectrophotometry was used to follow the Cu^{II}/Cu^{I} conversion. Initially, the characterization of these complexes by absorption spectrophotometry UV−visible was carried out in a mixture of PhMe:MeCN in a ratio 85:15 (see Supporting Information, Figure S1). The addition of two phen equivalents into a solution of the Cu^{I} salt ($Cu(MeCN)_4BF_4$) gave the [Cu^{I}(phen)$_2$]$^{+}$ complex. This compound exhibits a characteristic absorption band at λ_{max} = 444 nm (see Figure S1A). When 1 equiv of phen was used, two absorption bands at λ = 364 and 444 nm were observed. These bands correspond to two different complexes: [Cu^{I}(phen)]$^{+}$ and [Cu^{I}(phen)$_2$]$^{+}$. We additionally performed TD-DFT (PCM(ACN)-[M06/def2-TZVPP]) (see Computational Details) calculations to assign the absorption bands. The computed vertical excitations show two band absorptions at 251 and 428 nm for [Cu^{I}(phen)$_2$]$^{+}$ (see Tables S1−S2 and Figure S16A), where the latter is assigned to the metal-to-ligand charge-transfer (MLCT), in good agreement with former observations.[25] On the other hand, a weak absorption at 326 nm was obtained for [Cu^{I}(phen)]$^{+}$ (Tables S3−S4 and Figure S16C). However, when a second equivalent of ligand was added, only the band at λ = 444 nm was observed. In contrast, a solution of the Cu^{II} salt ($Cu(CF_3SO_3)_2$) with two equivalents of the ligand showed a broad absorption band at λ_{max} = 740 nm (calculated 529 and 651 nm), corresponding to the [Cu^{II}(phen)$_2$]$^{2+}$ complex (see Figure S1B and S16B and Tables S11 and S12). The experimental values of the absorption bands observed for Cu^{I} and Cu^{II} with phen in PhMe:MeCN (85:15) as solvent are consistent with values previously reported in DMF.[12b]

The sulfur nucleophile mediated Cu^{II}/Cu^{I} transformation was thus studied. Compound **1** was added to the previously formed solution of [Cu^{II}(phen)$_2$]$^{2+}$ complex, and the absorption of the system was followed over time (Figure S2). The absorption band of the [Cu^{II}(phen)$_2$]$^{2+}$ complex vanished, and a new signal at λ = 444 nm was observed. This signal corresponds to the characteristic absorption band of the [Cu^{I}(phen)$_2$]$^{+}$ complex, indicating Cu^{II} reduction into Cu^{I}.

It is also important to note that addition of **1** to Cu^{II} complex led to the rapid formation of an intermediate species, which has an absorption band at λ_{max} = 366 nm, and then evolved to [Cu^{I}(phen)$_2$]$^{+}$ complex (λ_{max}= 444 nm) (see Figure S2). The band at λ_{max} = 366 nm could correspond to [Cu^{I}phen]$^{+}$ complex (see Figure S1A) or [Cu^{I}(phen)Nu] (Figure 3B). Our calculations indicate that the absorption bands of [Cu^{I}(phen)Nu] are 422, 303, and 245 nm, overlapping with transition corresponding to [Cu^{I}(phen)$_2$]$^{+}$ and [Cu^{I}(phen)]$^{+}$. Subsequently, the Cu^{II}/Cu^{I} transformation was followed upon 2 h, and the Cu^{I} complex formed at λ = 444 nm (Figure 1) was quantified. The ε value for [Cu^{I}(phen)$_2$]$^{+}$ complex was estimated as 6300 cm^{-1} M^{-1}. After 2 h, 41% of the Cu^{I} complex was

DOI: 10.1021/acs.joc.7b01991
J. Org. Chem. 2017, 82, 11464−11473

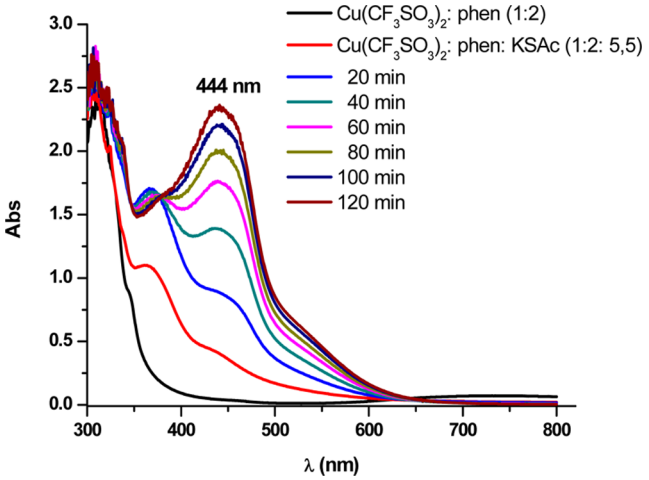

Figure 1. UV−vis spectra (1 cm UV cell) at room temperature. $[Cu^{II}(phen)_2]^{2+}$ generated from the mixing of $(Cu(CF_3SO_3)_2)$ (0.9 mM) and 1,10-phenanthroline (phen) (1.8 mM) in 3 mL of PhMe:MeCN, 85:15), (black curve). Addition of KSAc (**1**) (5 mM, 5.5 equiv) results in the appearance of $[Cu^{I}(phen)_2]^{+}$. The upper spectrum (brown curve) was obtained after 120 min.

obtained. This experiment was repeated using a different initial concentration of $[Cu^{II}(phen)_2]^{2+}$ (0.7 mM) complex, and similar results were obtained.

These experiments show that in situ sulfur nucleophile mediated reduction of Cu^{II} species into catalytically active Cu^{I} species occurs in a similar way as with alcohol and amine nucleophiles.[12b] In the present case, formation of the Cu^{I} complex from the reduction of Cu^{II} by KSAc is, however, less efficient than with phenoxide or phenyl amine anions.

Study and Characterization of the Complexes Involved at the Beginning of the Catalytic Cycle. *Electrochemical Characterization of the Components of the Catalyst System.* To study the complexes involved at the beginning of the catalytic cycle, we performed the electrochemical characterization of each component. We first used $Cu(MeCN)_4BF_4$ as copper source, phen as auxiliary ligand, PhI as electrophile, and KSAc as sulfur nucleophile (Figure S3). All CVs were performed in PhMe:MeCN (85:15) as solvent in the presence of 0.1 M TBATFB as supporting electrolyte. Table 1 summarizes the results.[24]

Table 1. Electrochemical Characterization of the Components in the Catalyst System[a]

species	type	E_p oxidation	E_p reduction
Cu^{I}/Cu^{II}	reversible	+1.09	+0.91
Cu^{I}/Cu^{0}	irreversible		−0.47
Cu^{0}/Cu^{I}	irreversible	+0.13	
phen	irreversible		−1.92
KSAc	irreversible	+0.44	
PhI	irreversible		−2.30

[a]Cyclic voltammetry at carbon-disk electrode (1 mm diameter) at a scan rate of 0.1 V s^{-1} performed in PhMe:MeCN (85:15) containing n-Bu_4NBF_4 (0.1M, TBATFB) as supporting electrolyte at 22 °C. All peak potentials are expressed in volts vs SCE.

The cyclic voltammogram of the Cu^{I} salt exhibits a reversible oxidation peak corresponding to the redox couple Cu^{I}/Cu^{II} (E^0 = 1.0 V vs SCE). The reduction peak at E_p = −0.47 V vs SCE is due to the formation of Cu^0, which is then deposited on the electrode surface. An oxidative, redissolution peak into Cu^{I} is observed at E_p = 0.13 V vs SCE. The cyclic voltammogram of the ligand (phen) is irreversible with a reduction peak at E_p = −1.92 V vs SCE. In the case of the salt KSAc (**1**), an irreversible oxidation wave with E_p = 0.44 V is obtained. Finally, the cyclic voltammogram of the electrophile shows an irreversible reduction signal at a potential E_p = −2.30 V vs SCE.

Electrochemical Characterization of Cu/Phen Complexes. It is well-known that phen species bind to Cu^{I} cation (eqs 1 and 2).[2S,12b] Therefore, we electrochemically characterized these complexes in PhMe:MeCN solvent mixture.

$$[Cu^{I}S_4]^{+} + \text{phen} \underset{}{\overset{K_1=5\times10^5}{\rightleftharpoons}} [\text{phen}Cu^{I}S_2]^{+}2S \quad (1)$$

$$[\text{phen}Cu^{I}S_2]^{+} + \text{phen} \underset{}{\overset{K_2=8\times10^4}{\rightleftharpoons}} [Cu^{I}\text{phen}S_2]^{+}2S$$

$$S = \text{MeCN};\ 20°C;\ \text{phen} = 1,10\text{-phenanthroline} \quad (2)$$

The CV of Cu^{I} was performed with 1 and 2 equiv of the ligand (Figure 2). By adding one equivalent of phen (relatively to Cu^{I}), two new oxidation signals were observed with E_p = 0.47 V and 0.63 vs SCE (Figure 2A). However, the corresponding oxidation wave of the free Cu^{I} cation (or solvated Cu^{I}, $[Cu^{I}S_4]^{+}$) could still be detected. Through addition of a second equivalent of the ligand (Figure 2B), the Cu^{I} signal vanishes and a free single oxidation wave appears (E_p = 0.33 V vs SCE), which corresponds to the oxidation of the complex $[Cu^{I}phen_2]^{+}$. These features indicate that the complex Cu^{I}/phen is more easily oxidized than the free Cu^{I} cation.

Reaction of $[Cu^{I}phen_2]^{+}$ Complex in PhMe/MeCN. Once the $[Cu^{I}(phen)_2]^{+}$ complex was characterized, its behavior was studied in the presence of different amounts of **1** (Figure 3). Upon addition of 2 or 3 equiv of **1**, two new oxidation waves E_p = 0.17 and 1.25 V vs SCE appeared in the CV (Figure 3A). The new oxidation signal at E_p = 0.17 V vs SCE could indicate the formation of a new complex ($[Cu^{I}(phen)Nu]$) with the participation of the nucleophile (Nu = AcS^{-}) to the coordination sphere. This observation was confirmed by UV−vis absorption spectrophotometry (Figure 3B). When the nucleophile was added to $[Cu^{I}(phen)_2]^{+}$ complex, the intensity of the absorption band at λ = 444 nm decreased, and a new band appeared at approximately λ = 370 nm. Therefore, the $[Cu^{I}(phen)_2]^{+}$ complex may not be present in reaction conditions where the nucleophile is in large excess with respect to the initial concentrations of Cu^{I} and phen.

The next step was to evaluate the effect of the addition of the electrophile (PhI) to the new $[Cu^{I}(phen)(SAc)]$ complex by CV and UV−vis spectrophotometry (see Supporting Information, Figure S4). During these experiments, the temperature of the medium was raised up to 40 °C to increase the solubility of the nucleophile in the solvent (PhMe/MeCN). Unfortunately, the addition of PhI did not produce any change in the oxidation signal of the $[Cu^{I}(phen)(SAc)]$ complex, and similar results were observed by UV−vis spectrophotometry (Figures S4A and B, respectively).

Then, the behavior of the complex $[Cu^{I}(phen)_2]^{+}$ was studied in the presence of the electrophile (PhI). After the addition of 1 and 2 equiv of PhI, no modification of the CV was observed, and no change was detected by UV−vis spectrophotometry (see Supporting Information, Figure S5). That is, under our experimental conditions, we could not observe reaction between the electrophilic species and the $[Cu^{I}(phen)_2]^{+}$ complex.

Finally, a solution of the Cu^{I} salt was prepared, and **1** was added to evaluate the possible formation of $[Cu^{I}(SAc)_2]^{-}$

DOI: 10.1021/acs.joc.7b01991
J. Org. Chem. 2017, 82, 11464−11473

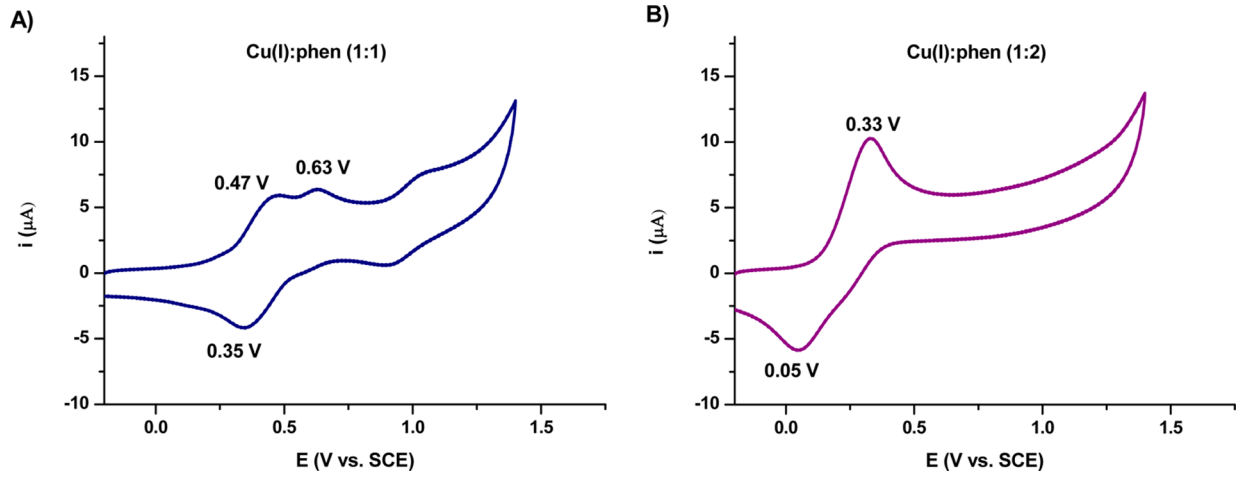

Figure 2. Cyclic voltammetry of a solution of $Cu(MeCN)_4BF_4$ (1 mM in PhMe:MeCN/TBATFB) at a glassy carbon-disk electrode (1 mm diameter) and a scan rate of 0.1 V s^{-1} at 20 °C in the presence of 1,10-phenanthroline (phen): (A) 1 and (B) 2 equiv.

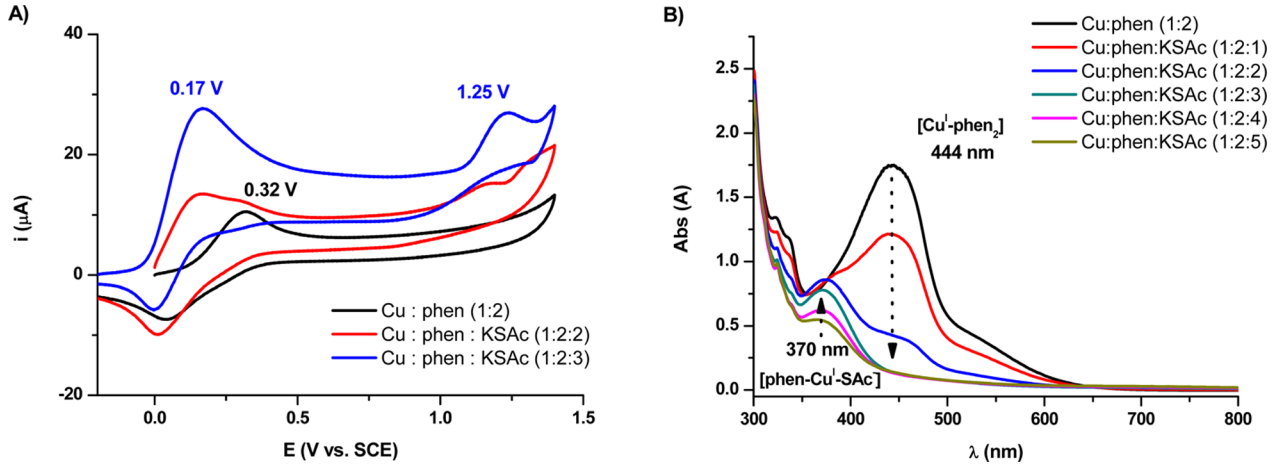

Figure 3. Reaction of $[Cu^I(phen)_2]^+$ complex by the addition of **1**. (A) CV for $[Cu^I(phen)_2]^+$ complex (1 mM, in PhMe:MeCN/TBATFB) and after the addition of **1** (2 and 3 mM) at a glassy carbon-disk electrode (1 mm diameter) and a scan rate of 0.1 V s^{-1} at 20 °C. (B) UV−vis spectrum from $[Cu^I(phen)_2]^+$ complex (0.2 mM, in PhMe:MeCN) and after the addition of **1** (from 0.2 to 1 mM).

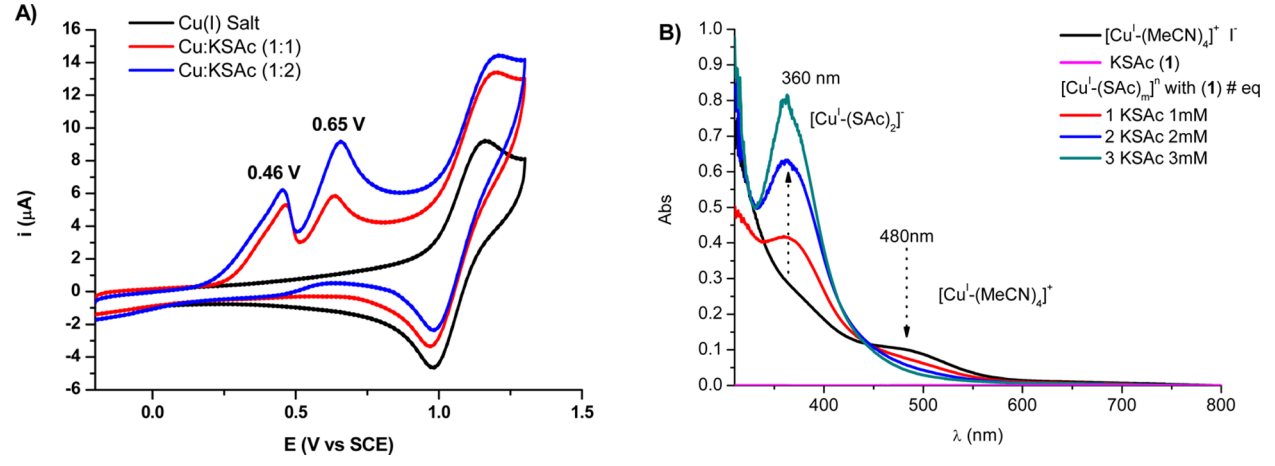

Figure 4. Reaction of $[Cu^I(MeCN)_4]^+$ complex by the addition of **1**. (A) CV of the $Cu(MeCN)_4BF_4$ complex (1 mM, in PhMe:MeCN/TBATFB) and after the addition of 1 and 2 equiv of **1** at a glassy carbon-disk electrode (1 mm diameter) and a scan rate of 0.1 V s^{-1} at 20 °C. (B) UV−vis spectra of the $[Cu^I(MeCN)_4]^+$ complex (CuI 1 mM in PhMe:MeCN, 85:15) and after addition of 1, 2, and 3 equiv of KSAc.

complex. CV revealed a new oxidation signal at E_p = 0.65 V vs SCE, accompanied by signals corresponding to Cu^I and **1** (Figure 4A). This new signal may indicate the formation of a complex between the metal and the nucleophile. Furthermore, a solution of $[Cu^I(MeCN)_4]^+$ in PhMe:MeCN (85:15) was prepared, and the UV−vis spectra shows an absorption band at

DOI: 10.1021/acs.joc.7b01991
J. Org. Chem. 2017, 82, 11464−11473

λ_{max} = 480 nm, which evolved to a new band at 360 nm after addition of **1**, assigned to the formation of the $[Cu^{I}(SAc)_2]^-$ complex (Figure 4B).

After the addition of 2 equiv of the phen ligand to a Cu^{I}:**1** mixture in a 1:1 ratio, an oxidation wave with E_p = 0.17 V vs SCE was observed, corresponding to the $[Cu^{I}(phen)(SAc)]$ complex, similarly to the signal previously detected and characterized (Figure 3). It could be due to the existence of an equilibrium between the complexes $[Cu^{I}(phen)(SAc)]$ and $[Cu^{I}(SAc)_2]^-$ in the reaction medium. To check for this equilibrium, the model reaction was carried out adding the copper source, the ligand, and the nucleophile salt (**1**) in different orders (reaction a = 1° Cu^{I}, 2° KSAc, 3° phen; reaction b = 1° KSAc, 2° Cu^{I}, 3° phen, etc.). After 24 h of reaction at 100 °C, no significant difference in product **2** yield was noticed. Although the reaction may form different complexes, they are all in equilibrium with a common intermediate, $[Cu^{I}(phen)(SAc)]$, which is likely the catalytically active species. In addition, we carried out in situ ESI-HRMS analysis to characterize possible Cu complex intermediates formed in toluene at room temperature (Figures S6–S9). The ESI-HRMS in the positive-ion mode showed a peak with m/z = 423.06 together with another peak with m/z = 318.98; the former was assigned to $[Cu^{I}(phen)_2]^+$, while the second was identified as $[Cu^{I}(phen)(SAc)+H]^+$. A third peak with m/z = 242.99 was also observed, which was assigned to $[Cu^{I}(phen)]^+$. These are the Cu species found under our experimental conditions in the positive-ion mode. Probably due to the slight solubility of Cu species in toluene at room temperature, the ion abundance determined for these species was low; consequently, the observed uncertainty was slightly high. Nevertheless, these observations show that $[Cu^{I}(phen)(SAc)]$ together with $[Cu^{I}(phen)_2]^+$ and $[Cu^{I}(phen)]^+$ are formed in the catalytic system at room temperature in good agreement with UV–vis and cyclic voltammetry characterization experiments discussed above.

Determination of the Aryl Halide Activation Step. While our results confirm the formation and participation of a precomplex $[Cu^{I}(phen)(SAc)]$, the activation step of the aryl halide may occur by different processes, such as HAT, SET, OA/RE, or σ-bond metathesis. To gain insight into the activation step, a series of experiments was performed.

Experimental Evidence for the Activation Pathway of the C–Halogen bond. During the electrochemical studies, it was not possible to observe the reaction between $[Cu^{I}(phen)(SAc)]$ complex (generated in situ) and PhI, at least under the conditions tested. This may be due to a large barrier for the activation step of the C–X bond, being rate-determining in the mechanism. It should be noted that these reactions occur at 100 °C and after 24 h in toluene as solvent. Although the diverse proposed mechanistic pathways involve different oxidation states of the metal, it is difficult to identify the oxidation state of Cu under the experimental conditions. However, the nature of the intermediates can be interpreted by using thoroughly designed experiments. To do so, remarkable ways to recognize free-radical intermediates have been described elsewhere.[12c,d,15d]

With this in mind, 1-(allyloxy)-2-iodobenzene (**3**) was employed as an electrophile and allowed to react with **1** for 24 h under catalytic conditions. If radicals were formed during the reaction, it would result in a rapid 5-*exo*-trig ring closure reaction to form a [3-(2,3,dihydrobenzofuran)]methyl radical with a rate constant of 9.6 × 10^9 s^{-1} in DMSO.[26] This radical would combine with the nucleophile or abstract atom hydrogen from the solvent. Only unrearranged product **4** (69% isolated yield) was formed from direct electrophilic substitution (Scheme 2), suggesting that free-aryl radicals are not intermediates in the reaction.

Scheme 2. Cu-Catalyzed Arylation Reaction of 1 with 1-(Allyloxy)-2-iodobenzene (3)

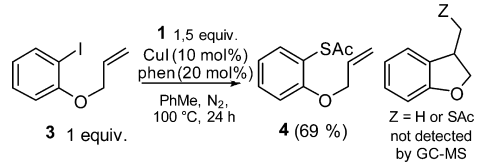

Moreover, it was previously reported that the photoinduced reaction of PhI with **1** in DMSO gives the PhSMe after quenching the crude reaction mixture with MeI (Scheme 3A).

Scheme 3. Cu- and Photo-Catalyzed Arylation Reactions of 1 with PhI

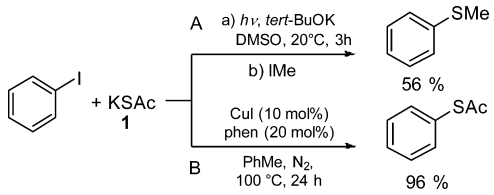

The participation of $S_{RN}1$-type mechanism was proposed, which involves fragmentation of the radical anion intermediate $[PhSAc]^{\bullet -}$ to gives benzenethiolate anion.[27] In contrast, the Cu-catalyzed reaction provides the PhSAc in excellent yields (Scheme 3B).[23] Such different behaviors observed clearly indicate that a different mechanism is operating in both reactions.

The use of dihalobenzenes allows testing for the intermediacy of aryl radical-anions species and the possible contribution of an $S_{RN}1$ mechanism.[28] Thus, we employed 1-bromo-4-iodobenzene (**5**) as an electrophile. It is known that bromobenzene did not react with **1** by Cu-catalysis under the experimental conditions, which means that the C_{Ar}–Br bond is not directly activated during the arylation reaction.[23] However, if the activation of C_{Ar}–I bond in **5** occurs by an SET or HAT processes, an aryl radical will be generated which, after coupling with the Nu, will form a radical anion. Once formed, this radical anion would react by intermolecular or more likely by intramolecular ET. Thus, cleavage of the C_{Ar}–Br bond would take place by an intramolecular ET, and the disubstituted product would be generated. However, the Cu-catalyzed reaction of **5** with **1** gave only the monosubstituted product (**6**) with retention of bromine in 80% yield (Scheme 4). Given the lack of C_{Ar}–Br

Scheme 4. Cu-Catalyzed Arylation Reaction of 1 with 1-Bromo-4-iodobenzene (5)

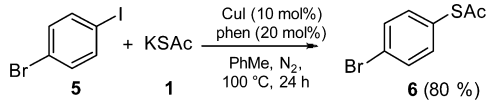

activation bond product and the lack of C_{Ac}–S fragmentation in **6**, the presence of radical anion intermediates can be ruled out.

Moreover, if the activating step of the C–X bond proceeds by an ET pathway, the same should occur from the initial

DOI: 10.1021/acs.joc.7b01991
J. Org. Chem. 2017, 82, 11464–11473

[Cu^{I}(phen)(SAc)]complex with the electrophile PhI. Considering the oxidation potential for the complex [Cu^{I}(phen)(SAc)] (E_p = 0.17 V vs SCE) and the reduction potential for PhI (E_p = −2.30 V vs SCE) in PhMe:MeCN, it suggests that an electron transfer would be highly endergonic. In other words, the transfer of an electron from the [Cu^{I}(phen)(SAc)] to PhI is thermodynamically very unfavorable and kinetically endowed with a high barrier (ΔG^{0}_{ET} and $\Delta G^{\ddagger}_{ET}$ close to 38 and 44 kcal mol^{-1}, respectively; see Supporting Information). Overall, the participation of free radicals during the C_{Ar}−I bond activation could be dismissed.

Computational Exploration of the Different Reaction Mechanism. To gain further insight into the operating mechanism, we carried out quantum chemical calculations at the PCM(PhMe)-[M06/def2-TZVPP] and PCM(MeCN)-[M06/def2-TZVPP] levels of theory. The thermodynamics between the different possible copper species in solution were first studied. As it was previously suggested,[12e,21,29] at least five species which are displayed in Scheme 5 may be formed. The complex [Cu^{I}I(phen)] can be produced by the direct mixing of CuI and phen. The computed dissociation Gibbs energy suggests a strong binding (ΔG = +35.8 and +33.8 kcal/mol in PhMe and MeCN, respectively). The addition of **1** and consequent release of KI is slightly endergonic (ΔG = +3.8 kcal/mol); [Cu^{I}(phen)(SAc)] can further disproportionate to generate the ionic species [Cu^{I}(phen)$_2$]$^+$ and [Cu^{I}(SAc)$_2$]$^-$. Similar phenomena were experimentally obtained by Fiaschi et al.[12e,30] and Chen et al.[15d] Indeed, Zhang et al. demonstrated that the formation of these complexes strongly depends on the nature of the solvent.[12f,21,31] We found this disproportionation is unfavorable by 22.7 kcal/mol in PhMe and by only 1.4 kcal/mol in MeCN, in good agreement with results obtained elsewhere.[12f,21,31] Interestingly, the dimerization is thermodynamically favorable by ΔG = −2.3 kcal/mol in PhMe and has almost no energy penalty in MeCN (ΔG = +0.6 kcal/mol). This result is in agreement with those reported by Weng et al.[22]

According to Scheme 5, the most stable species in PhMe is [Cu^{I}I(phen)], albeit under experimental conditions (i.e., a large excess of KSAc), [Cu^{I}(phen)(SAc)] is likely to be abundant. In MeCN, the five species [Cu^{I}I(phen)], [Cu^{I}(phen)(SAc)], [Cu^{I}(phen)(SAc)]$_2$, [Cu^{I}(phen)$_2$]$^+$, and [Cu^{I}(SAc)$_2$]$^-$ are predicted to be in equilibrium. In addition, it has been demonstrated that the most reactive species are [Cu^{I}I(phen)] and [Cu^{I}(phen)(SAc)].[12d,32] In this context, we calculated the energy barriers for all the most probable pathways for the formation of PhSAc (**2**) by considering both complexes as the reactive species toward PhI. We took into account commonly suggested mechanisms, namely oxidative addition/reductive elimination (OA/RE), σ-bond metathesis (MET), HAT, and SET.[4a,10d,14b,16] Figure 5 illustrates the computed Gibbs energy profile in PhMe and MeCN solution.

The single electron transfer from the [Cu^{I}(phen)(SAc)] complex to PhI forming the radical cation Cu^{II} and the formation of phenyl radical and I^- in both PhMe and MeCN was disregarded based on strong experimental evidence from cyclic voltammetry measurements that such pathway is not feasible. The so-called halogen atom transfer mechanism was proposed to occur in the reaction of *O*- and *S*-arylations of aryl halides.[12f,21] Here, **1** could transfer the iodine atom to the Cu^{I} center, leading to the formation of the complex [(phen)Cu^{II}SAcI] ($\mathbf{INT_{IAT}}$) and phenyl radical. The phenyl radical can later attack either the SAc moiety to form the product or the Cu^{II} center to yield a Cu^{III} species. DFT calculations predict a high energy lying intermediate for this pathway. The Gibbs energies relative to the separated reactants are 41.5 kcal/mol in PhMe and 40.1 kcal/mol in MeCN. This intermediate is about 10 kcal/mol less stable than the one reported for the catalytic cross-coupling between PhSH and PhI.[21] Unfortunately, all the attempts to locate the transition state ($\mathbf{TS_{IAT}}$) were unsuccessful. Instead, we estimated the barrier energy by the Marcus−Hush equation, which gave 43.1 and 41.9 kcal/mol for PhMe and MeCN, respectively (Figure 5, gray line).

The σ-bond metathesis reaction pathway was considered next. The transition state $\mathbf{TS_{MET}}$ consists in the concerted C−I bond breaking and C−S bond formation. The structure of the transition state is presented in Figure 5 (blue line). The four-membered transition state results in a strong energy demand, i.e., 45.2 and 46.7 kcal/mol in PhMe and MeCN, respectively. In contrast, OA/RE involves the same process but in a stepwise manner. The first step is the cleavage of the Ph−I bond via a three-membered transition state ($\mathbf{TS_{OA\text{-}1}}$), where the iodine atom takes an axial position while Ph takes an equatorial position. $\mathbf{TS_{OA\text{-}1}}$ is a late developing transition state, where the I−Ph distance is 2.536 Å. Remarkably, the activation barrier is only +26.2 kcal/mol above the reactants in PhMe and +27.3 kcal/mol in MeCN (Figure 5, black line). These values are lower than those computed for the related amide (+28.7 kcal/mol),[12e] PhOH (+34.2 kcal/mol),[12f] and PhSH (+39.3 kcal/mol)[21] arylation reactions. However, it is predicted to be slower than the trifluoromethylthiolation (+21.0 kcal/mol).[22] The resulting intermediates $\mathbf{INT_{OA/RE\text{-}1}}$ have energies of +23.9 and +24.7 kcal/mol, close to that of $\mathbf{TS_{OA\text{-}1}}$. The subsequent reductive elimination to yield **2** is strongly exergonic by 39.2 and 41.9 kcal/mol. The transition state ($\mathbf{TS_{RE\text{-}1}}$) is only 1.8 and 0.6 kcal/mol above the intermediate. Considering the thermochemical equilibrium indicated in Scheme 5, an alternative

Scheme 5. Equilibrium between the Possible Copper Species[a]

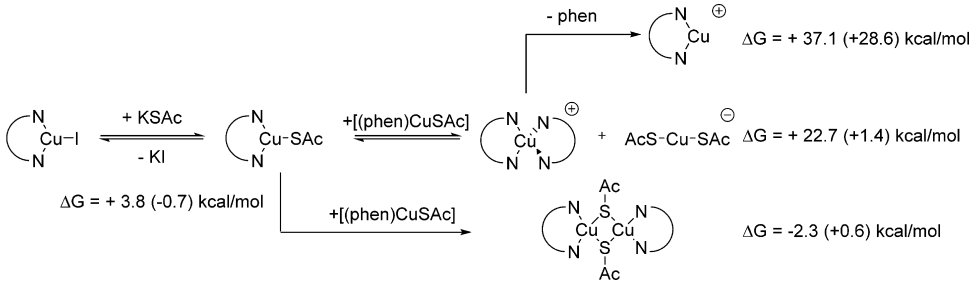

[a]The numbers are Gibbs free energy variations (ΔG, kcal/mol) computed at the PCM(PhMe)-[M06/def2-TZVPP] and PCM(MeCN)-[M06/def2-TZVPP] (in parentheses) levels of theory.

DOI: 10.1021/acs.joc.7b01991
J. Org. Chem. 2017, 82, 11464−11473

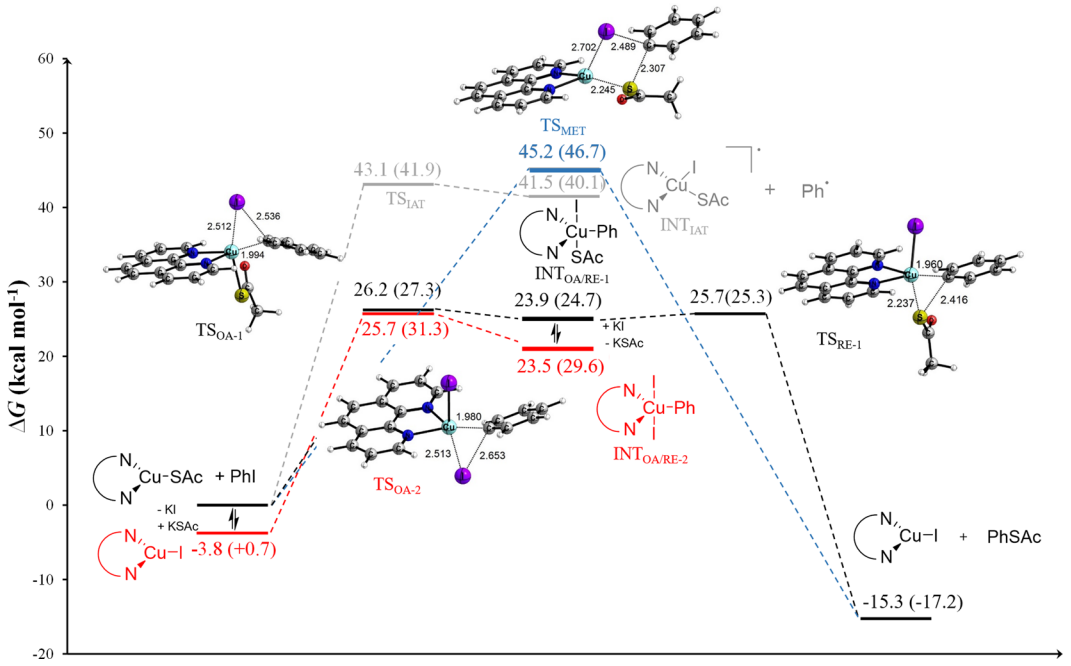

Figure 5. Computed Gibbs energy profile (ΔG at 298.15 K) of the Cu-catalyzed cross-coupling reaction between PhI and KSAc. OA/RE of [Cu^{I}(phen)(SAc)] (black line) and [Cu^{I}I(phen)] (red line), and MET (blue line) and iodine atom transfer (IAT/HAT) (gray line). Relative Gibbs energy and bond distances are given in kcal mol^{-1} and Å, respectively. All calculations were performed at the PCM(PhMe)-[M06/def2-TZVPP] and PCM(MeCN)-[M06/def2-TZVPP] (in parentheses) level of theory.

reaction pathway consists of the oxidative addition of **1** directly to the complex [Cu^{I}I(phen)], which results in the formation of the intermediate $\mathbf{INT_{OA/RE\text{-}2}}$. This intermediate lies just 0.4 kcal/mol below $\mathbf{INT_{OA/RE\text{-}1}}$ (in PhMe) and the barriers for its formation amounts to 29.5 kcal/mol (Figure 5, red line). From $\mathbf{INT_{OA/RE\text{-}2}}$, one I^{-} can be exchanged by $^{-}$SAc, leading to $\mathbf{INT_{OA/RE\text{-}1}}$, which then continues the reaction pathway to the final adduct. The energies shown in Figure 5 suggest that this process is possible in PhMe, while it is not feasible in MeCN (uphill by 4.9 kcal/mol).

The overall results indicate that the Cu-catalyzed cross-coupling reaction of thioacetate and iodobenzene would occur via an OA/RE reaction mechanism. The first transition state is the rate-determining step, leading to an unstable Cu^{III} intermediate which collapses into the products. It is worthy to mention that these results explain our unsuccessful attempts to detect the Cu^{III} intermediate. The energy profile in Figure 5 shows a highly unfavorable equilibrium to form the $\mathbf{INT_{OA/RE\text{-}1}}$ and a fast conversion into product. Thus, neither the thermodynamic nor the kinetic conditions are met for intermediate detection.[33]

CONCLUSIONS

We studied the mechanism of the Cu-catalyzed C–S cross-coupling reaction between thioacetate and PhI. Four different pathways were envisioned to explain the formation of phenyl thioacetate: single electron transfer, halogen atom transfer, oxidative addition/reductive elimination, and σ-bond metathesis. The following conclusions were drawn: (i) from UV–visible spectroscopy, it was demonstrated that Cu^{I} species are reactive species. (ii) Cyclic voltammetry studies indicate that the Cu^{I} species involved in the reaction can be oxidized more easily in the presence of phen as an auxiliary ligand. This feature might favor the catalytic cycle reaction. (iii) Through addition of KSAc to the $[Cu^{I}(phen)_2]^{+}$ complex, a new species was formed with a lower oxidation potential. (iv) Evidence against the formation of radical intermediates was obtained by performing a test reaction with radical clock probes and *p*-bromo iodobenzene. (v) DFT calculations indicate that the oxidative addition/reductive elimination presents the lowest activation barrier. The addition can be done from both [Cu^{I}I(phen)] and [Cu^{I}(phen)(SAc)] complexes.

EXPERIMENTAL SECTION

Materials and Methods. *Reactives and General Equipment.* All chemical reagents ($Cu(CF_3SO_3)_2$), $Cu(CH_3CN)_4BF_4$, CuI, CuCl, 1,10-phenantroline, potassium thioacetate, iodobenzene, tetrabuthylamonium tetrafluorborate ($^{n}Bu_4NBF_4$, TBATFB), 1-bromo-4-iodobenzene, 2-iodophenol, and allyl bromide were obtained commercially and used without further purification.

The compound 1-(allyloxy)-2-iodobenzene (**3**) was obtained from 2-iodophenol by reaction with allyl bromide, as described in the literature.[34]

General Methods. ^{1}H and ^{13}C NMR spectra were recorded at 400.16 and 100.62 MHz, and all spectra were reported in δ (ppm) relative to Me_4Si (solvent $CDCl_3$). Gas chromatographic analyses were performed on a chromatograph with a flame-ionization detector on 30 m capillary column of a 0.32 mm × 0.25 μm film thickness with a 5% phenylpolysiloxane phase. GC–MS analyses were performed on a spectrometer by electronic impact (70 eV) positive mode employing a 25 m × 0.2 mm × 0.33 μm with a 5% phenylpolysiloxane phase column. HRMS spectra were recorded on an orthogonal acceleration time-of-flight (oa-TOF) mass spectrometer. Ionization was achieved by ESI (positive detection mode).

Cyclic Voltammetry. Cyclic voltammetry of ($Cu(CF_3SO_3)_2$), $Cu(CH_3CN)_4BF_4$, 1,10-phenanthroline, KSAc, and PhI (0.1 mM solutions) was conducted in a three electrode glass cell thermostated at 25 °C under a dry nitrogen or argon atmosphere. The working electrode was a 1 mm diameter glassy carbon electrode. The electrode was carefully polished and ultrasonically rinsed with ethanol before each run. The reference electrode was a saturated calomel electrode (SCE) in a solution of MeCN/TBATFB (0.1 M) separated from the main

DOI: 10.1021/acs.joc.7b01991
J. Org. Chem. 2017, 82, 11464–11473

solution by a fine porosity glass frit. The counter electrode was a platinum wire.

The potentiostat was connected to a computer that recorded the current vs potential curves.[35] The scan rate used ranges from 0.1 to 100 V/s; all the CV presented in the figures were taken at 0.1 V/s. A feedback correction was applied to minimize the Ohmic drop between the working and reference electrodes.

General Procedure for CuI-Catalyzed C−S Arylation Reactions.[23] *Synthesis of S-2-(Allyloxy)-phenyl Thioacetate (4) and S-4-Bromophenylthioacetate (6).* A 10 mL two-necked Schlenk tube, equipped with magnetic stirrer and nitrogen inlet, was first dried with heat gun and under vacuum. Once cooled, 4 mL of PhMe, degassed under an N_2 stream for 20 min, was added. Then, ArX (0.5 mmol), CuI (10 mol %, 0.05 mmol), 1,10-phenanthroline (20 mol %, 0.1 mmol), and finally KSAc (1.5 equiv., 0.75 mmol) were added under N_2 atmosphere. The reaction mixture was heated at 100 °C for 24 h, cooled at room temperature, poured into ethyl ether (20 mL) and water (20 mL), and the mixture was stirred. The organic phase was separated, and the aqueous phase was extracted with 2 aliquots of ethyl ether (20 mL). The organic phases were combined and dried over anhydrous Na_2SO_4 and filtered. The crude reaction product was analyzed by GC and GC−MS. The products were isolated by column chromatography or radial chromatography or were quantified by GC with internal standard method.

In Situ High Resolution ESI-MS Characterization of Cu Complex Intermediates. A toluene solution of KSAc (1.5 equiv), IPh (1.0 equiv), CuI (10 mol %), and 1,10-phenanthroline (phen, 20 mol %) was stirred at room temperature for 2 h under N_2 atmosphere, the same experimental conditions used in the general procedure for CuI-catalyzed C−S arylation reactions, and ESI-HRMS analysis of the reaction was performed.

Computational Details. Geometry optimizations were performed using the Gaussian 09 optimizer[36] together with Turbo Mole V7.0.[37] All geometry optimizations were computed using the functional M06[38] in combination with the def2-TZVPP basis set.[39] The stationary points were located with the Berny algorithm[40] using redundant internal coordinates. Analytical Hessians were computed to determine the nature of stationary points (one and zero imaginary frequencies for transition states and minima, respectively)[41] and to calculate unscaled zero-point energies (ZPEs) as well as thermal corrections and entropy effects using the standard statistical−mechanics relationships for an ideal gas.[42] Transition structures (TSs) show only one negative eigenvalue in their diagonalized force constant matrices, and their associated eigenvectors were confirmed to correspond to the motion along the reaction coordinate under consideration using the intrinsic reaction coordinate (IRC) method.[43] Unless otherwise stated, Gibbs energies were computed at 298.15 K. For these calculations, the PhMe and MeCN solvents were described by nonspecific solvent effects within the self-consistent reaction field (SCRF) approach in Tomasi's formalism.[44]

Time-dependent density functional theory (TDDFT) was employed to calculate excitation energies as implemented in ORCA 4.0.1.2.[45] We used the functionals M06,[38] B3LYP,[46] CAM-B3LYP,[47] and PBE0[48] in combination with the def2-TZVPP basis sets. The solvent MeCN was described in this case by the conductor-like polarizable continuum model, CPCM.[49]

Characterization of Isolated Compounds. All products were characterized by ^{1}H NMR, ^{13}C NMR, and GC−MS. The following compounds are known, and their signals are in agreement with data previously reported in the literature: 1-(allyloxy)-2-iodobenzene (**3**),[33] *S*-phenyl thioacetate (**2**),[50] and *S*-(4-bromophenyl) thioacetate (**6**).[51]

S-(2-(Allyloxy)phenyl) Thioacetate (4). The typical above-described procedure was followed using 1-(allyloxy)-2-iodobenzene (**3**, 0.5 mmol), CuI (10 mol %, 0.05 mmol), 1,10-phenanthroline (20 mol %, 0.1 mmol), and KSAc (1.5 equiv, 0.75 mmol). After extraction, the crude residue was purified by column chromatography using pentane/CH_2Cl_2 (75/25) as solvent mixture to afford pure **4** as an oily liquid (71.9 mg, 69%). ^{1}H NMR ($CDCl_3$) δ 7.41−7.35 (m, 2H); 7.01−6.94 (m, 2H); 6.01 (ddt, J = 17.2; 10.5; 4.9 Hz, 1H, H-10); 5.41 (ddd, J = 17.2; 3.3; 1.6 Hz, 1H); 5.27 (ddd, J = 10.5; 2.9; 1.5 Hz, 1H); 4.58 (dt, J = 4.9; 1.6 Hz, 2H, H_2-9); 2.40 (s, 3H, H_3-8). ^{13}C NMR ($CDCl_3$) δ 193.5 (C, CO-7); 158.2 (C, C-6); 136.6; 132.8; 131.5; 121.3; 117.40; 116.9 (C, C-1); 113.1; 69.4 (CH_2, C-9); 30.0 (CH_3, C-8). GC−MS (m/z) 208 (M^+, 14), 167 (11), 166 (100), 165 (8), 151 (25), 137 (44), 133 (15), 125 (52), 119 (8), 97 (33), 96 (13), 70 (10), 69 (10), 43 (56), 41 (25). ESI-HRMS m/z $[M + Na]^+$ calcd for $C_{11}H_{12}NaO_2S$ 231.0450, found 231.0452.

■ ASSOCIATED CONTENT

Supporting Information

The Supporting Information is available free of charge on the ACS Publications website at DOI: 10.1021/acs.joc.7b01991.

Electrochemical, UV−vis spectroscopic, and HRMS characterization of reaction components; experimental evaluation of E_a for the ET pathway; Cartesian coordinates and energies; and ^{1}H NMR and ^{13}C NMR for compound **4** (PDF)

■ AUTHOR INFORMATION

Corresponding Authors

*E-mail: penenory@fcq.unc.edu.ar; Phone: (+54) 351-5353867.

*E-mail: diego.andrada@uni-saarland.de.

ORCID

Marc Robert: 0000-0001-7042-4106

Alicia B. Peñéñory: 0000-0001-9557-6472

Notes

The authors declare no competing financial interest.

■ ACKNOWLEDGMENTS

The authors acknowledge ECOS-Sud (Grant A10E03), INFIQC−CONICET, and Universidad Nacional de Córdoba (UNC). This work was supported partly by MINCyT-ECOS, Consejo Nacional de Investigaciones Científicas y Técnicas (CONICET), and Fondo de Ciencia y Tecnología (FONCYT), Argentina. S.M.S.-C. gratefully acknowledges the receipt of a fellowship from CONICET.

■ DEDICATION

This paper is dedicated to the memory of Adriana Beatriz Pierini, 1953−2016.

■ REFERENCES

(1) (a) Beletskaya, I. P.; Ananikov, V. P. *Chem. Rev.* **2011**, *111*, 1596−1636. (b) Shen, C.; Zhang, P.; Sun, Q.; Bai, S.; Hor, T. S. A.; Liu, X. *Chem. Soc. Rev.* **2015**, *44*, 291−314. (c) McReynolds, M. D.; Dougherty, J. M.; Hanson, P. R. *Chem. Rev.* **2004**, *104*, 2239−2258. (d) Mellah, M.; Voituriez, A.; Schulz, E. *Chem. Rev.* **2007**, *107*, 5133−5209. (e) Murphy, A. R.; Frechet, J. M. J. *Chem. Rev.* **2007**, *107*, 1066−1096. (f) Evano, G.; Theunissen, C.; Pradal, A. *Nat. Prod. Rep.* **2013**, *30*, 1467−1489.

(2) (a) Kondo, T.; Mitsudo, T.-a. *Chem. Rev.* **2000**, *100*, 3205−3220. (b) Lee, C.-F.; Liu, Y.-Ch; Badsara, S. S. *Chem. - Asian J.* **2014**, *9*, 706−722. (c) Bichler, P.; Love, J. A.; Vigalok, A. *Top. Organomet. Chem.* **2010**, *31*, 39.

(3) (a) Beletskaya, I. P.; Cheprakov, A. V. *Coord. Chem. Rev.* **2004**, *248*, 2337−2364. (b) Ley, S. V.; Thomas, A. W. *Angew. Chem., Int. Ed.* **2003**, *42*, 5400−5449. (c) Monnier, F.; Taillefer, M. *Angew. Chem., Int. Ed.* **2008**, *47*, 3096−3099. (d) Ma, D.; Cai, Q. *Acc. Chem. Res.* **2008**, *41*, 1450−1460.

(4) (a) Sperotto, E.; van Klink, G. P. M.; van Koten, G.; de Vries, J. G. *Dalton Trans.* **2010**, *39*, 10338−10351. (b) Monnier, F.; Taillefer, M. *Angew. Chem., Int. Ed.* **2009**, *48*, 6954−6971. (c) Evano, G.; Blanchard, N.; Toumi, M. *Chem. Rev.* **2008**, *108*, 3054−3131.

DOI: 10.1021/acs.joc.7b01991
J. Org. Chem. 2017, 82, 11464−11473

(d) Finet, J. P.; Fedorov, A. Y.; Combes, S.; Boyer, G. *Curr. Org. Chem.* **2002**, *6*, 597−626.
(5) (a) Evindar, G.; Batey, R. A. *J. Org. Chem.* **2006**, *71*, 1802−1808. (b) Beletskaya, I. P.; Sigeev, A. S.; Peregudov, A. S.; Petrovskii, P. V. *Mendeleev Commun.* **2006**, *16*, 250−251. (c) Ding, Q.; He, X.; Wu, J. *J. Comb. Chem.* **2009**, *11*, 587−591. (d) Wang, F.; Chen, C.; Deng, G.; Xi, C. *J. Org. Chem.* **2012**, *77*, 4148−4151.
(6) (a) Baskin, J. M.; Wang, Z. *Org. Lett.* **2002**, *4*, 4423−4425. (b) Herrero, M. T.; San Martín, R.; Domínguez, E. *Tetrahedron* **2009**, *65*, 1500−1503. (c) Prasad, D. J. C.; Sekar, G. *Org. Lett.* **2011**, *13*, 1008−1011.
(7) (a) Ma, D.; Geng, Q.; Zhang, H.; Jiang, Y. *Angew. Chem., Int. Ed.* **2010**, *49*, 1291−1294. (b) Gan, J.; Ma, D. *Org. Lett.* **2009**, *11*, 2788−2790. (c) Zhu, W.; Ma, D. *J. Org. Chem.* **2005**, *70*, 2696−2700.
(8) (a) Lv, X.; Bao, W. *J. Org. Chem.* **2007**, *72*, 3863−3867. (b) Xu, H.-J.; Zhao, X.-Y.; Deng, J.; Fu, Y.; Feng, Y. S. *Tetrahedron Lett.* **2009**, *50*, 434−437.
(9) (a) Palomo, C.; Oiarbide, H.; López, R.; Gómez-Bengoa, E. *Tetrahedron Lett.* **2000**, *41*, 1283−1286. (b) Kumar, S.; Engman, L. *J. Org. Chem.* **2006**, *71*, 5400−5403.
(10) (a) Verma, A. K.; Singh, J.; Chaudhary, R. *Tetrahedron Lett.* **2007**, *48*, 7199−7202. (b) Rout, L.; Saha, P.; Jammi, S.; Punniyamurthy, T. *Eur. J. Org. Chem.* **2008**, *2008*, 640−643. (c) Feng, Y.; Wang, H.; Sun, F.; Li, Y.; Fu, X.; Jin, K. *Tetrahedron* **2009**, *65*, 9737−9741. (d) Sambiagio, C.; Marsden, S. P.; Blacker, A. J.; McGowan, P. C. *Chem. Soc. Rev.* **2014**, *43*, 3525−3550.
(11) (a) Weingarten, H. *J. Org. Chem.* **1964**, *29*, 3624−3626. (b) Cohen, T.; Cristea, I. *J. Am. Chem. Soc.* **1976**, *98*, 748−753. (c) Paine, A. J. *J. Am. Chem. Soc.* **1987**, *109*, 1496−1502.
(12) (a) Mansour, M.; Giacovazzi, R.; Ouali, A.; Taillefer, M.; Jutand, A. *Chem. Commun.* **2008**, 6051−6053. (b) Franc, G.; Jutand, A. *Dalton Trans.* **2010**, *39*, 7873−7875. (c) Tye, J. W.; Weng, Z. Q.; Giri, R.; Hartwig, J. F. *Angew. Chem., Int. Ed.* **2010**, *49*, 2185−2189. (d) Tye, J. W.; Weng, Z.; Johns, A. M.; Incarvito, C. D.; Hartwig, J. F. *J. Am. Chem. Soc.* **2008**, *130*, 9971−9983. (e) Zhang, S.-L.; Liu, L.; Fu, Y.; Guo, Q.-X. *Organometallics* **2007**, *26*, 4546−4554. (f) Zhang, S.; Zhu, Z.; Ding, Y. *Dalton Trans.* **2012**, *41*, 13832−13840.
(13) (a) Eichman, C. C.; Stambuli, J. P. *Molecules* **2011**, *16*, 590−608. (b) Yu, H.; Zhang, M. S.; Li, Y. Z. *J. Org. Chem.* **2013**, *78*, 8898−8903. (c) Ma, D.; Xie, S.; Xue, P.; Zhang, X.; Dong, J.; Jiang, Y. *Angew. Chem., Int. Ed.* **2009**, *48*, 4222−4225.
(14) (a) Casitas, A.; Ribas, X. In *Copper-Mediated Cross-Coupling Reactions*; John Wiley & Sons, Inc.: Hoboken, NJ, 2013; p 239;. (b) Casitas, A.; Ribas, X. In *Copper-Mediated Cross-Coupling Reactions*; John Wiley & Sons, Inc.: Hoboken, NJ, 2013; p 253. (c) Casitas, A.; Canta, M.; Sola, M.; Costas, M.; Ribas, X. *J. Am. Chem. Soc.* **2011**, *133*, 19386−19386. (d) Huffman, L. M.; Stahl, S. S. *J. Am. Chem. Soc.* **2008**, *130*, 9196−9197.
(15) (a) Huffman, L. M.; Casitas, A.; Font, M.; Canta, M.; Costas, M.; Ribas, X.; Stahl, S. S. *Chem. - Eur. J.* **2011**, *17*, 10643−10650. (b) Casitas, A.; King, A. E.; Parella, T.; Costas, M.; Stahl, S. S.; Ribas, X. *Chem. Sci.* **2010**, *1*, 326−330. (c) Giri, R.; Hartwig, J. F. *J. Am. Chem. Soc.* **2010**, *132*, 15860−15863. (d) Chen, C. H.; Weng, Z. Q.; Hartwig, J. F. *Organometallics* **2012**, *31*, 8031−8037.
(16) (a) Jones, G. O.; Liu, P.; Houk, K. N.; Buchwald, S. L. *J. Am. Chem. Soc.* **2010**, *132*, 6205−6213. (b) Bowman, W. R.; Heaney, H.; Smith, P. H. G. *Tetrahedron Lett.* **1984**, *25*, 5821−5824.
(17) Fier, P. S.; Hartwig, J. F. *J. Am. Chem. Soc.* **2012**, *134*, 10795−10798.
(18) (a) Bacon, R. G. R.; Hill, H. A. O. *J. Chem. Soc.* **1964**, 1097−1119. (b) Bacon, R. G. R.; Karim, A. *J. Chem. Soc., Perkin Trans. 1* **1973**, 272−280.
(19) Weingarten, H. *J. Org. Chem.* **1964**, *29*, 977−978.
(20) Cheng, S.-W.; Tseng, M.-C.; Lii, K.-H.; Lee, C.-R.; Shyu, S.-G. *Chem. Commun.* **2011**, *47*, 5599−5601.
(21) Zhang, S.-L.; Fan, H.-J. *Organometallics* **2013**, *32*, 4944−4951.
(22) Weng, Z. Q.; He, W. M.; Chen, C. H.; Lee, R.; Tan, D.; Lai, Z. P.; Kong, D. D.; Yuan, Y. F.; Huang, K. W. *Angew. Chem., Int. Ed.* **2013**, *52*, 1548−1552.
(23) (a) Soria-Castro, S. M.; Peñéñory, A. B. *Beilstein J. Org. Chem.* **2013**, *9*, 467−475. (b) Soria-Castro, S. M.; Bisogno, F.; Peñéñory, A. B. *Org. Chem. Front.* **2017**, *4*, 1533−1540.
(24) It was not possible to use pure toluene as a solvent to solubilize the ionic species such as TBATFB, the Cu salt, and **1**.
(25) Meyer, M.; Albrecht-Gary, A. M.; Dietrich-Buchecker, C. O.; Sauvage, J. P. *Inorg. Chem.* **1999**, *38*, 2279−2287.
(26) Annunziata, A.; Galli, C.; Marinelli, M.; Pau, T. *Eur. J. Org. Chem.* **2001**, *2001*, 1323−1329.
(27) Schmidt, L. C.; Rey, V.; Peñéñory, A. B. *Eur. J. Org. Chem.* **2006**, *2006*, 2210−2214.
(28) Rossi, R. A.; Pierini, A. B.; Peñéñory, A. B. *Chem. Rev.* **2003**, *103*, 71−167.
(29) Yu, H.-Z.; Jiang, Y.-Y.; Fu, Y.; Liu, L. *J. Am. Chem. Soc.* **2010**, *132*, 18078−18091.
(30) Fiaschi, P.; Floriani, C.; Pasquali, M.; Chiesivilla, A.; Guastini, C. *Inorg. Chem.* **1986**, *25*, 462−469.
(31) Zhang, S. L.; Bie, W. F.; Huang, L. *Organometallics* **2014**, *33*, 5263−5271.
(32) Zhang, S. L.; Ding, Y. Q. *Organometallics* **2011**, *30*, 633−641.
(33) Bernasconi, C. F. *Investigation of rates and mechanisms of reactions, general considerations and reactions at conventional rates*; Wiley-Interscience: Hoboken, NJ, 1986; Vol. *6*.
(34) Boisvert, G.; Giasson, R. *Tetrahedron Lett.* **1992**, *33*, 6587−6590.
(35) Pause, L.; Robert, M.; Saveant, J. M. *J. Am. Chem. Soc.* **1999**, *121*, 7158−7159.
(36) Frisch, M. J.; Trucks, G. W.; Schlegel, H. B.; Scuseria, G. E.; Robb, M. A.; Cheeseman, J. R.; Scalmani, G.; Barone, V.; Mennucci, B.; Petersson, G. A.; Nakatsuji, H.; Caricato, M.; Li, X.; Hratchian, H. P.; Izmaylov, A. F.; Bloino, J.; Zheng, G.; Sonnenberg, J. L.; Hada, M.; Ehara, M.; Toyota, K.; Fukuda, R.; Hasegawa, J.; Ishida, M.; Nakajima, T.; Honda, Y.; Kitao, O.; Nakai, H.; Vreven, T.; Montgomery, J. A.; Peralta, J. E.; Ogliaro, F.; Bearpark, M.; Heyd, J. J.; Brothers, E.; Kudin, K. N.; Staroverov, V. N.; Kobayashi, R.; Normand, J.; Raghavachari, K.; Rendell, A.; Burant, J. C.; Iyengar, S. S.; Tomasi, J.; Cossi, M.; Rega, N.; Millam, J. M.; Klene, M.; Knox, J. E.; Cross, J. B.; Bakken, V.; Adamo, C.; Jaramillo, J.; Gomperts, R.; Stratmann, R. E.; Yazyev, O.; Austin, A. J.; Cammi, R.; Pomelli, C.; Ochterski, J. W.; Martin, R. L.; Morokuma, K.; Zakrzewski, V. G.; Voth, G. A.; Salvador, P.; Dannenberg, J. J.; Dapprich, S.; Daniels, A. D.; Farkas, O.; Foresman, J. B.; Ortiz, J. V.; Cioslowski, J.; Fox, D. J. Gaussian 09, revision C.01; Gaussian, Inc.: Wallingford CT, 2009.
(37) TURBOMOLE V7.0 2015, a development of University of Karlsruhe and Forschungszentrum Karlsruhe GmbH, 1989−2007, TURBOMOLE GmbH, since 2007; available from http://www.turbomole.com.
(38) Zhao, Y.; Truhlar, D. G. *Theor. Chem. Acc.* **2008**, *120*, 215−241.
(39) (a) Schäfer, A.; Horn, H.; Ahlrichs, R. *J. Chem. Phys.* **1992**, *97*, 2571−2577. (b) Weigend, F.; Ahlrichs, R. *Phys. Chem. Chem. Phys.* **2005**, *7*, 3297−3305.
(40) Peng, C. Y.; Ayala, P. Y.; Schlegel, H. B.; Frisch, M. J. *J. Comput. Chem.* **1996**, *17*, 49−56.
(41) McIver, J. W., Jr; Komornicki, A. *J. Am. Chem. Soc.* **1972**, *94*, 2625−2633.
(42) Atkins, P. W.; De Paula, J. *Physical Chemistry*, 8th ed.; Oxford University Press: Oxford, New York, 2006.
(43) Gonzalez, C.; Schlegel, H. B. *J. Phys. Chem.* **1990**, *94*, 5523−5527.
(44) (a) Miertus, S.; Scrocco, E.; Tomasi, J. *Chem. Phys.* **1981**, *55*, 117−129. (b) Barone, V.; Cossi, M.; Tomasi, J. *J. Comput. Chem.* **1998**, *19*, 404−417.
(45) Neese, F. *Orca-an ab initio, density functional and semiempirical program package*, 4.0.1.2; Max-Planck Institute for Bioinorganic Chemistry: Mulheim an der Ruhr, Germany, 2005.
(46) (a) Becke, A. D. *Phys. Rev. A: At., Mol., Opt. Phys.* **1988**, *38*, 3098−3100. (b) Lee, C.; Yang, W.; Parr, R. G. *Phys. Rev. B: Condens. Matter Mater. Phys.* **1988**, *37*, 785−789.

DOI: 10.1021/acs.joc.7b01991
J. Org. Chem. 2017, 82, 11464−11473

(47) Yanai, T.; Tew, D. P.; Handy, N. C. *Chem. Phys. Lett.* **2004**, *393*, 51−57.
(48) Adamo, C.; Barone, V. *J. Chem. Phys.* **1999**, *110*, 6158−6170.
(49) Barone, V.; Cossi, M. *J. Phys. Chem. A* **1998**, *102*, 1995−2001.
(50) Qiu, R. H.; Xu, X. H.; Li, Y. H.; Shao, L. L.; Zhang, G. P.; An, D. L. *Synth. Commun.* **2010**, *40*, 3309−3314.
(51) Giri, S. K.; Gour, R.; Kartha, K. P. R. *RSC Adv.* **2017**, *7*, 13653−13667.

DOI: 10.1021/acs.joc.7b01991
J. Org. Chem. 2017, 82, 11464−11473